

Integrated optics for astronomical interferometry

P.V.S. Marques^{a,b}, A. Ghasempour^d, D. Alexandre^{a,b,c}, A.M.P Leite^b, P.J.V. Garcia^e, F. Reynaud^f

^aUnidade de Optoelectrónica e Sistemas Electrónicos – INESC Porto, Portugal

^bDepartamento de Física e Astronomia da Faculdade de Ciências da Universidade do Porto, Portugal

^cDepartamento de Física da Universidade de Trás-os-Montes e Alto Douro, Portugal

⁴Current address: Tennessee State University, Nashville, USA

^eDepartamento de Engenharia Física da Faculdade de Engenharia da Universidade do Porto, Portugal

^fXLIM département photonique/ IRO, 87060 Limoges cedex, France

ABSTRACT

Integrated optics is a well established technology that finds its main applications in the fields of optical communication and sensing. However, it is expanding into new areas, and in the last decade application in astronomical interferometry has been explored. In particular, several examples have been demonstrated in the areas of beam control and combination. In this paper, different examples of application integrated optics devices for fabrication of beam combiners for astronomical interferometry is given. For the multiaxial beam combiners, a UV laser direct writing unit is used for mask fabrication. The operation principles of the coaxial combiners fabricated in hybrid sol-gel were validated using an interferometric set-up. These results demonstrate that hybrid sol-gel technology can produce quality devices, opening the possibility of rapid prototyping of new designs and concepts.

Keywords: Interferometry, integrated optics, waveguides, astronomical optics

1. INTRODUCTION

Guided wave optics has been widely used in astronomical interferometry, starting with the use of optical fibers in many instruments. Fibers can be simply be used for optical signal transportation, but also for more complex functions that involve spatial filtering [1], optical coupling and interference [2]. Fiber components also find applications in this domain; fiber Bragg gratings are used to filter atmospheric collected radiation such the one that has origin on OH emission [3].

The other example of guided wave optics come from the application of integrated optics in instrumentation, which can be used for several applications such as tracking, beam combination and photometry, dispersive functions and detection [4]. Probably the most common application is beam combination, which is a fundamental function in long baseline astronomical interferometry. The complex visibility of the interferometric signal can be used to determine the object intensity distribution through Fourier processing according to the Van-Cittert Zernike theorem.

Integrated optic devices for application in astronomical interferometry have been demonstrated in several fabrication techniques. One is ion-exchange [5], where the refractive index increase in the designed areas is achieved with recourse to ion exchange between the salt and the glass substrate. Passive devices were also produced in silica technology using typical dry-etching structuring [6]. UV written devices were also demonstrated in germanium doped silica, showing two telescopes beam combination for the H-band [7]. Active devices were also demonstrated with recourse to Ti in-diffusion in periodically poled lithium niobate [8], where frequency up-conversion was demonstrated bringing the optical detection to visible wavelengths, taking advantage of the high quality of the detectors in this region (low noise and high quantum efficiency).

2. DESIGN AND FABRICATION

2.1 Optical design

The design of the prototypes of coaxial and multiaxial beam combiners for the J band (centered at $1.2 \mu\text{m}$) was done using a BPM-CAD commercial software package (Optiwave). Monomode channel waveguides were designed with a square core (typically $4 \times 4 \mu\text{m}^2$). Elements such as S-bends, X-crossings, Y-junctions and waveguide tapers were individually studied and optimized.

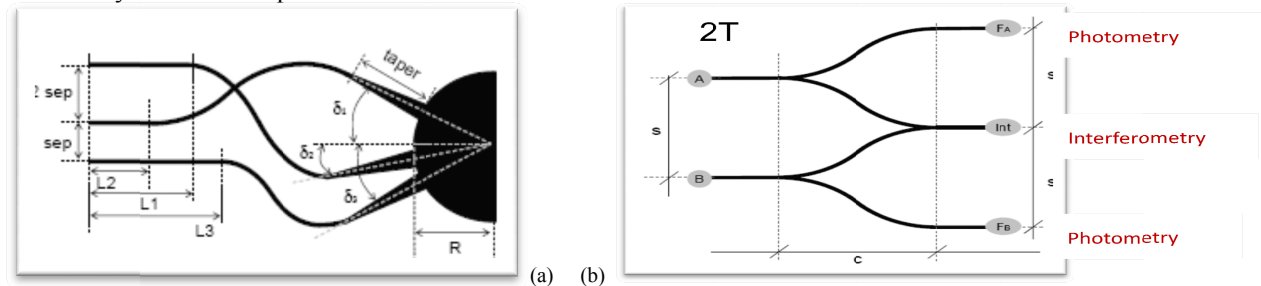


Figure 1. Schematic representation of (a) multiaxial and (b) co-axial integrated optic beam combiners for astronomical interferometry.

Figure 1a shows the layout of a multiaxial two beam combiner. Waveguide tapers are employed to achieve adiabatic expansion of the square core channel waveguide field to the fundamental mode of a rectangular core waveguide at the taper end ($150 \times 4 \mu\text{m}^2$), in order to ensure nearly collimated beams in the planar waveguide section. The radius R of the planar waveguide region and the angular separation of the taper ends must ensure that no coupling occurs between neighbour waveguides.

Figure 1b shows a coaxial two beam combiner, with photometry outputs, based on Y-junctions. For an even number N of input beams, the design of a coaxial all-in-one beam combiner follows almost directly from the design for $N=2$. However, in the case of N odd, the design is slightly more complex, as it is of fundamental importance to ensure that all interfering optical paths have the same optical length for correct spectral broadband operation.

In an all-in-one combiner all the baselines are multiplexed on the same output channel. This will result in a complex interferogram shape; the visibility and phase information of each combination pair can be extracted by Fourier analysis of the time dependent interferogram. To separate information in the Fourier space, the input beams should be time modulated using a non-redundant configuration. Feeding all the three inputs together was not possible due to set-up limitations, so each pair of inputs was tested individually.

2.2 Fabrication

The hybrid sol-gel technology offers an interesting potential for simplified fabrication and rapid prototyping of integrated optic devices, as low temperature processing is used, thick optical layers can be achieved in a single deposition and no reactive ion-etching (RIE) is needed [9,10]. Using the MAPTMS- ZrO_2 material system and UV laser patterning, channel waveguides and devices have been demonstrated, without recourse to photoinitiator [8]. The general fabrication procedure is shown in figure 2.

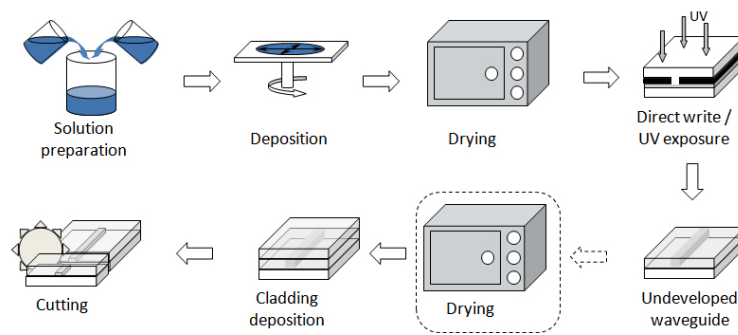


Figure 2. Fabrication steps for fabrication integrated optic devices in hybrid sol-gel technology.

Two different device production processes were used in the case of the results shown here. In the first case, the hybrid sol-gel material is exposed through an amplitude mask; the photopolymerized zones that will be the future waveguide cores will remain attached to the substrate, while the non-polymerized areas are simply washed away by an appropriate solvent. The structure is just covered with a cladding after development. Alternatively, the sample is just hard baked after UV exposure without development. On this case a refractive index contrast still is maintained between the exposed and non-exposed areas.

A laser direct writing system has been developed and used for producing photolithographic masks for fabrication of the multiaxial beam combiners and also for direct writing of coaxial beam combiners. The laser writer is computer controlled, uses the output CAD files from the integrated optics simulation package, and the pattern is written by X-Y displacement of crossed precision translation stages (2nm resolution) under the dynamically focused laser beam.

Loss levels measured on single mode sol-gel channel waveguides are 0.4dB/cm at 1300 nm, which are acceptable from the point of view of rapid prototyping. High performance devices should, however, employ lower loss silica waveguides which have a higher performance and their design follows very similar rules to those applied in the sol-gel case.

3. RESULTS

The devices fabricated were tested with the set-up shown in figure 3.

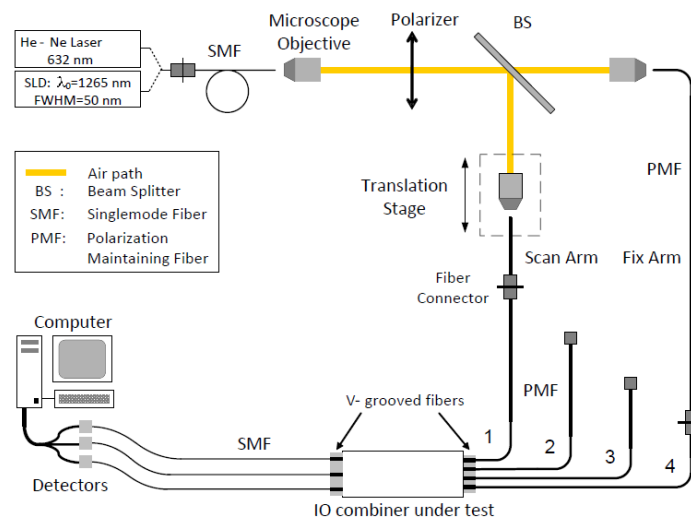


Figure 3. Experimental test set-up for characterization of integrated optics beam combiners..

The set-up has three different light sources available. The visible laser (He-Ne) is used for device alignment with optical fibres. The superluminescent diode (SLD) with a FWHM of 50nm and centered at 1265nm is used for the beam combiners characterization. The narrowband source at 1300 nm is used for loss characterization and modal characterization of the fabricated waveguides. The polarization is controlled before splitting and the Mach-Zehnder testing interferometer is made of a combination of free space propagation and guided wave through polarization maintaining fibers. A translation stage is used in one of the arms to balance the optical path between both arms and to measure the interferometric output as a function of path scanning. Please note that the fiber ribbons that couples light into the device has several fibers mounted in a silicon V-grooved chip. The beam combiners are tested pairwise and therefore the fiber connections have to be set according. In Figure 3 the system is set to acquire the interferogram between inputs 1 and 4 of a four telescope beam combiner (4T). For each pair of inputs, the normalized interferogram intensity is given by

$$I_c = \frac{I_{ij} - \alpha P_i - \beta P_j}{2\sqrt{\alpha P_i \beta P_j}} \quad (1)$$

It allows the correction of the bias induced by the photometric unbalance over the different interferometric arms. The normalized interferogram intensity calculation consists of several steps:

- I. Feeding both inputs i and j ($i \neq j$) and measuring the raw outputs: photometry P_i , photometry P_j and interferometry I_{ij} .
- II. Compute the interferometric to photometric ratios α and β . This is achieved by feeding only one input (T_i) at a time and measuring the interferometric (I_{i0}) and the photometric (P_{i0}) intensities. $\alpha = I_{i0}/P_{i0}$ is computed when input i is fed and $\beta = I_{j0}/P_{j0}$ when input j is fed.

Once the normalized intensity is computed using Eq. (1), the fringe visibility is estimated through

$$V = \frac{I_c^{\max} - I_c^{\min}}{2} \quad (2)$$

In the case of the multiaxial beam combiners, the output optical fibers and detectors are replaced with a vidicon camera and an optical imaging system that images the power distribution at the device output over the camera detector.

For easier characterization of the multiaxial two beam combiner (M2BC), a Y-splitter was added in the input of the device in the design of the photolithographic mask (see top of figure 4). This way only one input beam is required to test the whole device. Any path difference in the chip will appear as shifting of the brightest fringe from the center of the pattern. The M2BC have a length of 10 mm and the result of simulation shows that for this length, only 90% of the total power exists in the fundamental mode (better values can be achieved at the cost of extra length). Fig. 4b (bottom right) shows the fringes with visibility of 90% measured in the M2BC using the SLD as the source. The asymmetry in the envelope of the interference pattern is due to the excitation of higher modes in the tapered waveguide, due to non-optimal design.

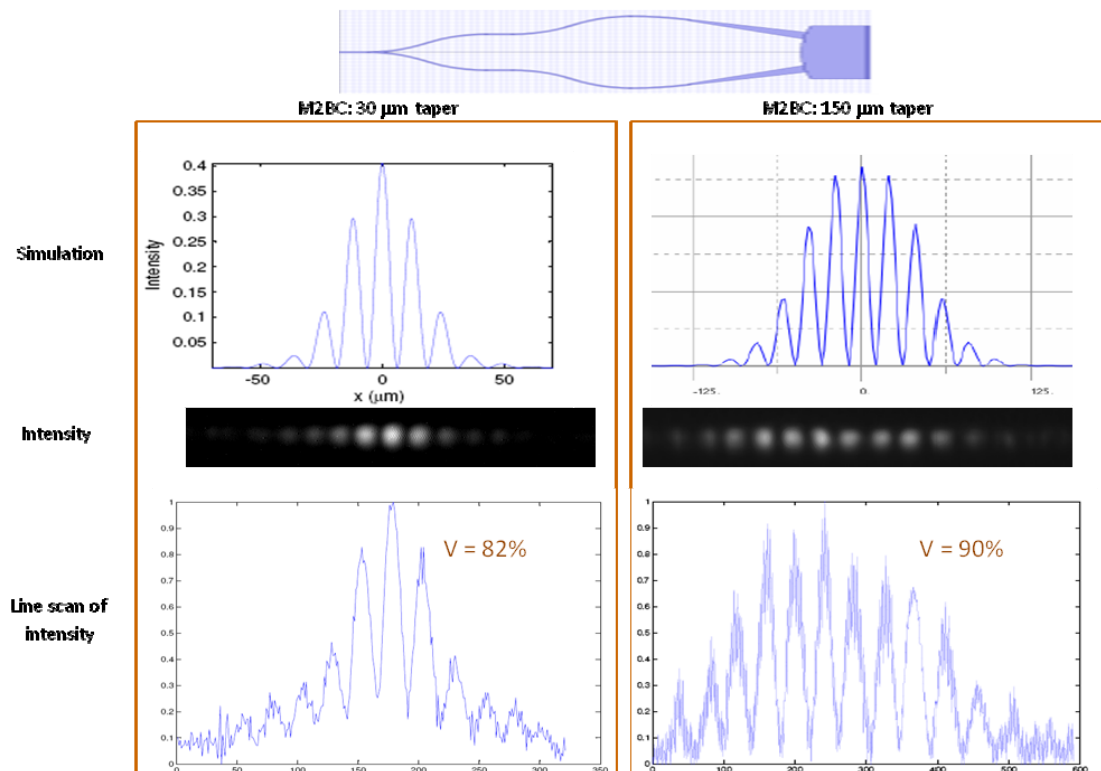


Figure 4. Simulation and experimental results for a two beam multiaxial beam combiner. Top) Device geometry and simulated spatial interferogram, middle) intensity profiles acquired with the vidicon camera and bottom) intensity profile at a horizontal scan line of the intensity profile.

Fringe visibility of 98% has been measured for the simplest coaxial two beam combiner. Figure 5c shows the normalized interferograms and respective visibilities for each combination pair of the coaxial three beam combiners. Fringe visibilities of 94%, 96% and 97% have been measured, respectively for the combination pairs 1-3, 2-3 and 1-2. The different visibility values can be related to different lengths of the input fibers, which can lead to residual different chromatic differential dispersions. The cross-talk in the X-junction between inputs T_2 and T_3 was determined by measuring P_{2b} (see figure), while only T_3 was fed, obtaining a value less than -27 dB (0.2%).

A four telescope beam combiner chip was also fabricated, being the best visibility between pair 1-2 ($V=97.5\%$) and the worst visibility value between pair 1-4 ($V=92.1\%$).

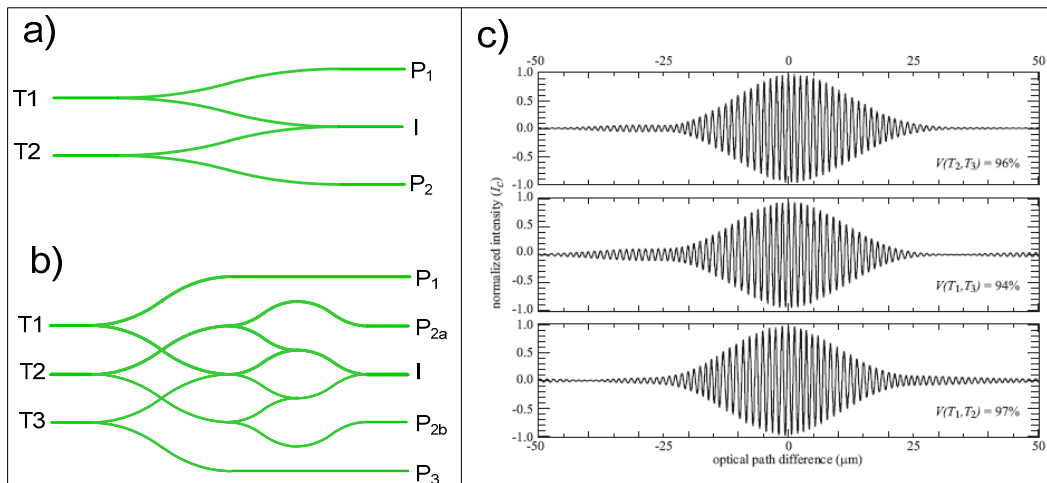


Figure 5. a-b) A coaxial two and three beam combiner geometries, respectively; c) Interferograms resulting from the pairwise combination in the coaxial three beam combiner.

The devices described above were produced following the steps described in figure 2, which employs flood exposure through an amplitude mask defined in a pure silica substrate. After exposure, the non photopolymerised areas are simply washed away and the waveguides core obtained by this process are subsequently covered by a cladding layer of hybrid sol-gel deposited after. However, devices can be produced by laser direct writing with a focused laser beam. In our case we used a frequency doubled argon laser emitting at 244nm. However, instead of using development of the non-polymerised areas we just applied thermal treatment to cure all the sol-gel. This process is useful for rapid prototyping as mask replication techniques are dispensable. Using this process two (2T) and three beam (3T) combiners were fabricated. Figure 6 shows a concatenation and stitching of photographs taken from a two beam combiner produced by the method described above; for this device the visibility was 95.1%, slightly below but comparable to the values obtained with devices produced with more standard techniques. However, when the number of inputs increase there was a clear degradation of the visibility values measured due to imperfections within the integrated chip. Figure 7 shows the visibility values obtained for the three beam combiners. It is obvious that there are some distortions of the interferograms as a consequence of errors within the device.



Figure 5. Coaxial two beam combiner obtained by photographs stitching.

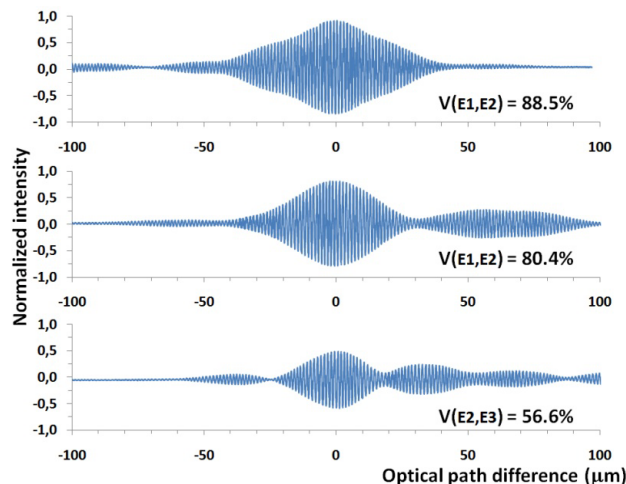


Figure 5. Normalized and corrected interferograms obtained from the interferometric output of the three beam combiner. The obtained fringe visibility was 88.5%, 80.4% and 56.6% for the (E1, E2), (E1, E3) and (E2, E3) pairs, respectively.

4. CONCLUSION

In this paper, the results of design, fabrication and characterization of a coaxial and multiaxial combiner and beam combiners for astronomical interferometry, using hybrid sol-gel technology are given. High contrast ($\geq 90\%$) fringes have been obtained, demonstrating the high performance of the devices made by hybrid sol-gel. We have recently developed a laser photopatterning system which allows the writing of devices with fast turnaround times, but the results indicated that a fine tuning of the fabrication process still is required, as the results obtained demonstrate a lower performance of the devices produced by this method.

REFERENCES

- [1] R. G. Petrov, F. Malbet, G. Weigelt, et. al., "AMBER, the near-infrared spectro-interferometric three-telescope VLTI instrument," *Astron Astrophys.* **464**, 1–12 (2007).
- [2] V. Coude du Foresto, P. J. Borde, A. Merand, C. Baudouin, A. Remond, G. S. Perrin, S. T. Ridgway, T. A. ten Brummelaar, and H. A. McAlister, "FLUOR fibered beam combiner at the CHARA array," in *Interferometry for Optical Astronomy II*, W. A. Traub, ed., Proc. SPIE **4838**, 280–285 (2003).
- [3] J. Bland-Hawthorn, M. Englund, and G. Edvell, "New approach to atmospheric OH suppression using an aperiodic fibre Bragg grating," *Opt. Express* **12**, 5902–5909 (2004).
- [4] F. Malbet, P. Kern, I. Schanen-Duport, J.-P. Berger, K. Rousset-Perraut, and P. Benech, "Integrated optics for astronomical interferometry. I. Concept and astronomical applications," *Astron. Astrophys. Suppl.* **138**, 135–145, (1999).
- [5] J. P. Berger, K. Rousset-Perraut, P. Kern, F. Malbet, I. Schanen-Duport, F. Reynaud, P. Haguenaer, and P. Benech, "Integrated optics for astronomical interferometry. II. First laboratory white-light interferograms," *Astron. Astrophys. Suppl.* **139**, 173–177 (1999).
- [6] LeBouquin, J.B., et al.: Integrated optics for astronomical interferometry VI. Coupling the light of the VLTI in K band, *Astronomy & Astrophysics*, 450(3): p. 1259-1264, 2006.
- [7] M. Olivero, M. Svalgaard, L. Jocou, and J.-P. Berger, "Direct UV-Written Integrated Optical Beam Combiner for Stellar Interferometry," *J. Lightwave Technol.* **25**, 367–371 (2007).
- [8] S. Brustlein, L. Del Rio, A. Tonello, L. Delage, F. Reynaud, H. Herrmann, and W. Sohler, "Laboratory Demonstration of an Infrared-to-Visible Up-Conversion Interferometer for Spatial Coherence Analysis," *Phys. Rev. Lett.* **100**, 153903-1–153903-4 (2008).
- [9] P. J. Moreira, P. V. S. Marques, A. P. Leite, "Hybrid sol-gel channel waveguide patterning using photoinitiator-free materials", *IEEE Photon. Technol. Lett.*, vol.17, No.2, pp. 399-401 (2005).